

## Functionalized BODIPY with various sensory units – a versatile colorimetric and luminescent probe for pH and ions†

Zhendong Yin,<sup>a,b</sup> Anthony Yiu-Yan Tam,<sup>b</sup> Keith Man-Chung Wong,<sup>b</sup> Chi-Hang Tao,<sup>b</sup> Bao Li,<sup>a</sup> Chun-Ting Poon,<sup>b</sup> Lixin Wu<sup>a</sup> and Vivian Wing-Wah Yam<sup>\*a,b</sup>

Received 24th February 2012, Accepted 13th July 2012

DOI: 10.1039/c2dt30446e

A series of BODIPY (4,4-difluoro-4-bora-3a,4a-diaza-s-indacene) derivatives containing ion- and pH-sensory units have been successfully designed and synthesized. One of the compounds was structurally characterized by X-ray crystallography. Owing to the presence of an ICT absorption band, one of the compounds was found to show pronounced solvatochromic behavior in different organic solvents. Their emission energies in various solvents show a linear dependence on the Lippert solvent parameter. The cation-binding properties of the complexes with different metal ions (alkali metal, alkaline earth metal and transition metal ions) have been studied using UV-vis and emission spectroscopies. A 1 : 1 complexation to metal ions (Li<sup>+</sup>, Na<sup>+</sup>, Mg<sup>2+</sup>, Ba<sup>2+</sup>, Zn<sup>2+</sup>, Cd<sup>2+</sup>) was found for the compound with one azacrown moiety in acetonitrile while another one with two azacrown moieties was shown to form 1 : 2 complexes with Zn<sup>2+</sup> and Mg<sup>2+</sup> cations. Their stability constants have been determined by both UV-vis and emission spectrophotometric methods. By introducing triarylborane moieties into the *meso* position and the 2-position of the BODIPY skeleton, different electronic absorption spectral changes together with an emission diminution were observed in response to fluoride ions. Ditopic binding study of **5**, which was functionalized with both azacrown and triarylborane moieties, showed emission enhancement in the presence of Mg<sup>2+</sup> and F<sup>-</sup>. These findings suggest that these BODIPY derivatives are capable of serving as versatile colorimetric and luminescence probes for pH, cations and F<sup>-</sup>.

## Introduction

Host–guest interactions have received much attention since the turn of the last century.<sup>1</sup> Most of the attention has been focused on the design of suitable host molecules based on host–guest interactions for highly selective molecular recognition. Especially for ions and molecules, the recognition and sensing process is of great importance in chemistry, biology, physiology, and environmental science. In recent years there has been a growing interest in the study of molecular probes for metal ions, such as alkali metal ions<sup>2</sup> and transition metal ions.<sup>3</sup> For example, sodium ion is considered as an essential element<sup>4</sup> and classified as a “dietary inorganic macro-mineral” for animals<sup>5</sup> due to the involvement of signal transmission of nerve impulses. Neuromodulation of electrical excitability is a fundamental mechanism in many aspects of learning, memory, and

physiological regulation. Voltage-gated Na<sup>+</sup> channels are responsible for the initiation and propagation of action potentials.<sup>6</sup>

Fluorescent dyes have been widely studied in the past several decades in many fields, such as in biological imaging,<sup>7</sup> chemosensing,<sup>8</sup> and molecular switching.<sup>9</sup> The coordination compounds of boron(III) have attracted recent attention<sup>10,11</sup> for the design and synthesis of new fluorescent dyes. In particular, BODIPY is one of the families of the widely used fluorescent dyes.<sup>12,13</sup> Because of their remarkable optical properties, including high absorption coefficients, narrow emission bands, high emission quantum yields and high photostability, they have been frequently used in biological labeling and sensing. Herein, we report the design, synthesis and spectroscopic studies of a series of BODIPY derivatives with various sensory units. Drastic color and spectral changes have been observed by the variation of pH value as well as in the presence of various ions. Ditopic binding properties of a BODIPY derivative with azacrown and triarylborane moieties have also been studied.

## Experimental section

## Materials and reagents

Tetra-*n*-butylammonium perchlorate, lithium perchlorate, sodium perchlorate, magnesium(II) perchlorate, barium(II) perchlorate,

<sup>a</sup>State Key Laboratory of Supramolecular Structure and Materials and College of Chemistry, Jilin University, Changchun 130012, P.R. China

<sup>b</sup>Institute of Molecular Functional Materials (Areas of Excellence Scheme, University Grants Committee (Hong Kong)) and Department of Chemistry, The University of Hong Kong, Pokfulam Road, Hong Kong. E-mail: wwyam@hku.hk

† Electronic supplementary information (ESI) available. CCDC 867744 (1). For ESI and crystallographic data in CIF or other electronic format see DOI: 10.1039/c2dt30446e

zinc(II) perchlorate, and cadmium(II) perchlorate were obtained from Aldrich Chemical Co. Acetonitrile was distilled over calcium hydride before use. All other reagents and solvents were of analytical grade and were used as received. 2-Methylpyrrole was prepared according to reported procedures.<sup>14</sup> 4,4-Difluoro-8-(4-hydroxyphenyl)-3,5-dimethyl-4-bora-3a,4a-diaza-*s*-indacene, 4,4-difluoro-8-(4-bromophenyl)-3,5-dimethyl-4-bora-3a,4a-diaza-*s*-indacene and 4,4-difluoro-8-phenyl-3,5-dimethyl-4-bora-3a,4a-diaza-*s*-indacene were synthesized according to reported procedures.<sup>15</sup> **Safety Note. Caution!** Metal perchlorate salts are potentially explosive. Only small amounts of these materials should be handled and with great caution.

## Syntheses

The synthetic pathway of compounds **1–5** is shown in Scheme 1. **1** and **2** were synthesized according to a modification of a literature procedure.<sup>16</sup> 4,4-Difluoro-8-(4-hydroxyphenyl)-3,5-dimethyl-4-bora-3a,4a-diaza-*s*-indacene (321 mg, 1 mmol) and 4-formyl-*N*-phenylaza-15-crown-5 (323 mg, 1 mmol) were dissolved in dry toluene (50 mL). Piperidine (0.5 mL) and acetic acid (0.5 mL) were then added to the mixture. The reaction mixture was heated to reflux in the presence of molecular sieves for 24 h. After cooling to room temperature, the solvent was then removed under reduced pressure to afford the crude product containing **1** and **2**, which were purified by column chromatography on silica gel using ethyl acetate–petroleum ether (from 3 : 1 to 4 : 1 v/v) as an eluent to give compounds **1** (154 mg, 25% yield) and **2** (166 mg, 18% yield).

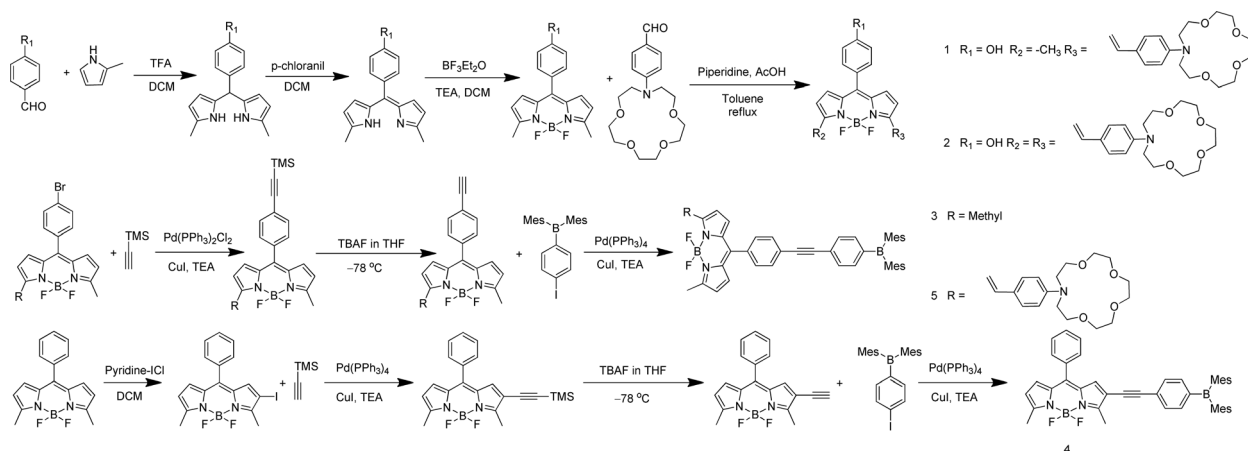
**1:** <sup>1</sup>H NMR (500 MHz, CDCl<sub>3</sub>, 298 K, relative to Me<sub>4</sub>Si)/ppm: δ = 2.65 (s, 3H; –CH<sub>3</sub>), 3.60–3.70 (m, 16H; –OCH<sub>2</sub>CH<sub>2</sub>N– and –OCH<sub>2</sub>CH<sub>2</sub>O–), 3.80 (t, 4H; –OCH<sub>2</sub>CH<sub>2</sub>N–), 5.60 (s, br, 1H; –OH), 6.25 (d, *J* = 3.95 Hz, 1H; pyrrole proton at 1-position), 6.65 (t, 3H; pyrrole protons at 7-position and 5'-*m*-Ar), 6.80 (d, *J* = 4.5 Hz, 1H; pyrrole proton at 6-position), 6.85 (d, *J* = 4.5 Hz, 1H; pyrrole proton at 1-position), 6.90 (d, *J* = 8.31 Hz, 2H; 8-*m*-Ar), 7.25 (d, *J* = 16.1 Hz, 1H; vinyl proton at 5'-position), 7.35 (d, *J* = 8.24 Hz, 2H; 8-*o*-Ar), 7.45 (d, *J* = 8.59 Hz, 2H; 5'-*o*-Ar), 7.50 (d, *J* = 16.1 Hz, 1H; vinyl proton at 5-position).

MS (EI<sup>+</sup>): *m/z*: 617.2; Anal. Calcd (%) for C<sub>34</sub>H<sub>38</sub>·BF<sub>2</sub>N<sub>3</sub>O<sub>5</sub>: C, 66.13; H, 6.20; N, 6.81; found: C, 66.37; H, 6.34; N, 6.71.

**2:** <sup>1</sup>H NMR (500 MHz, CDCl<sub>3</sub>, 298 K, relative to Me<sub>4</sub>Si)/ppm: δ = 3.60–3.70 (m, 32H; –OCH<sub>2</sub>CH<sub>2</sub>N– and –OCH<sub>2</sub>CH<sub>2</sub>O–), 3.80 (t, 8H; –OCH<sub>2</sub>CH<sub>2</sub>N–), 6.70 (d, *J* = 8.9 Hz, 4H; 3',5'-*m*-Ar), 6.75 (d, *J* = 4.4 Hz, 2H; pyrrole protons at 2,6-position), 6.85 (d, *J* = 4.4 Hz, 2H; pyrrole protons at 1,7-position), 6.90 (d, *J* = 8.6 Hz, 2H; 8-*o*-Ar), 7.20 (d, *J* = 16.0 Hz, 2H; vinyl protons at 3',5'-position), 7.35 (d, *J* = 8.6 Hz, 2H; 8-*m*-Ar), 7.50 (d, *J* = 8.9 Hz, 4H; 3',5'-*o*-Ar), 7.60 (d, *J* = 16.0 Hz, 2H; vinyl protons at 3,5-position). MS (EI<sup>+</sup>): *m/z*: 923.0; Anal. Calcd (%) for C<sub>51</sub>H<sub>61</sub>·BF<sub>2</sub>N<sub>4</sub>O<sub>9</sub>·0.5(EtOH): C, 66.03; H, 6.82; N, 5.92; found: C, 66.08; H, 6.69; N, 5.64.

**4,4-Difluoro-8-(4-trimethylsilylethynylphenyl)-3,5-dimethyl-4-bora-3a,4a-diaza-*s*-indacene.** A mixture of 4,4-difluoro-8-(4-bromophenyl)-3,5-dimethyl-4-bora-3a,4a-diaza-*s*-indacene (3.2 g, 8.56 mmol), trimethylsilylacetylene (6 mL, 42.78 mmol), CuI (81 mg, 0.43 mmol) and [Pd(PPh<sub>3</sub>)<sub>2</sub>Cl<sub>2</sub>] (300 mg, 0.43 mmol) in triethylamine (30 mL) was stirred and heated to reflux under nitrogen overnight. After removal of the solvents under reduced pressure, the residue was purified *via* silica gel chromatography (petroleum ether–dichloromethane 3 : 1 v/v) to give the desired product as a red solid (2.25 g, 67%). <sup>1</sup>H NMR (400 MHz, CDCl<sub>3</sub>, 298 K, relative to Me<sub>4</sub>Si)/ppm: δ = 0.27 (s, 9H; –CH<sub>3</sub>), 2.65 (s, 6H; –CH<sub>3</sub>), 6.27 (d, *J* = 4.1 Hz, 2H; pyrrole protons at 2,6-position), 6.67 (d, *J* = 4.1 Hz, 2H; pyrrole protons at 1,7-position), 7.43 (d, *J* = 8.4 Hz, 2H; 8-*o*-Ar), 7.56 (d, *J* = 8.4 Hz, 2H; 8-*m*-Ar).

**4,4-Difluoro-8-(4-ethynylphenyl)-3,5-dimethyl-4-bora-3a,4a-diaza-*s*-indacene.** 4,4-Difluoro-8-(4-trimethylsilylethynylphenyl)-3,5-dimethyl-4-bora-3a,4a-diaza-*s*-indacene (216 mg, 0.55 mmol) was dissolved in degassed THF (30 mL). Tetra-*n*-butylammonium fluoride (0.66 mL, 1 M in THF) was injected slowly at –78 °C. The reaction mixture was stirred at –78 °C for 30 min. After evaporation of the solvent, the residue was re-dissolved in dichloromethane (30 mL) and washed with deionized water twice (20 mL × 2). The organic layer was dried over anhydrous sodium sulfate. Subsequent filtration and removal of the solvent yielded the crude product, which was then purified by flash



Scheme 1 Synthetic route for the target molecules **1–5**.

column chromatography on silica gel using dichloromethane–petroleum ether (5 : 1 v/v) as an eluent to give the pure product (245 mg, 90%).  $^1\text{H}$  NMR (400 MHz,  $\text{CDCl}_3$ , 298 K, relative to  $\text{Me}_4\text{Si}$ )/ppm:  $\delta$  = 2.65 (s, 6H;  $-\text{CH}_3$ ), 3.21 (s, 1H;  $-\text{C}\equiv\text{CH}$ ), 6.28 (d,  $J$  = 4.1 Hz, 2H; pyrrole protons at 2,6-position), 6.68 (d,  $J$  = 4.1 Hz, 2H; pyrrole protons at 1,7-position), 7.46 (d,  $J$  = 8.2 Hz, 2H; 8-*o*-Ar), 7.60 (d,  $J$  = 8.2 Hz, 2H; 8-*m*-Ar).

**3:** To a solution of 4,4-difluoro-8-(4-ethynylphenyl)-3,5-dimethyl-4-bora-3a,4a-diaza-*s*-indacene (200 mg, 0.62 mmol),  $[\text{Pd}(\text{PPh}_3)_4]$  (46 mg, 0.4 mmol) and  $\text{CuI}$  (7.6 mg, 0.4 mmol) in  $\text{Et}_3\text{N}$  (40 mL) was added 4-iodophenyldimesitylborane (367 mg, 0.81 mmol). The reaction mixture was stirred under reflux for 16 h. After evaporation of the solvent under reduced pressure, the residue was purified by flash column chromatography on silica gel using dichloromethane–hexane (1 : 5 v/v) as an eluent to give **3** (130 mg, 31%) as an orange solid.  $^1\text{H}$  NMR (400 MHz,  $\text{CDCl}_3$ , 298 K, relative to  $\text{Me}_4\text{Si}$ )/ppm:  $\delta$  = 2.00 (d, 12H;  $-\text{CH}_3$ ), 2.32 (s, 6H;  $-\text{CH}_3$ ), 2.66 (s, 6H;  $-\text{CH}_3$ ), 6.28 (d,  $J$  = 4.2 Hz, 2H; pyrrole protons at 2,6-position), 6.72 (d,  $J$  = 4.1 Hz, 2H; pyrrole protons at 1,7-position), 6.84 (s, 4H; mesityl), 7.46–7.55 (m, 6H;  $-\text{C}_6\text{H}_4-$ ), 7.64 (d,  $J$  = 8.2 Hz, 2H;  $-\text{C}_6\text{H}_4-$ ). MS ( $\text{EI}^+$ ):  $m/z$ : 644.65; Anal. Calcd (%) for  $\text{C}_{43}\text{H}_{40}\text{B}_2\text{F}_2\text{N}_2$ : C, 80.14; H, 6.26; N, 4.35; found: C, 80.37; H, 6.11; N, 4.12.

**4,4-Difluoro-8-phenyl-2-iodo-3,5-dimethyl-4-bora-3a,4a-diaza-*s*-indacene.** 4,4-Difluoro-8-phenyl-3,5-dimethyl-4-bora-3a,4a-diaza-*s*-indacene (500 mg, 1.7 mmol) and pyridinium iodochloride (491 mg, 2.0 mmol) were dissolved in degassed dichloromethane (200 mL). The reaction mixture was stirred under  $\text{N}_2$  in the dark overnight. Upon quenching by addition of deionized water, the organic layer was extracted with dichloromethane and dried over anhydrous sodium sulfate. After subsequent filtration and solvent evaporation, the residue was purified by flash column chromatography on silica gel using dichloromethane–hexane (1 : 5 v/v) as an eluent to give the product as a red solid (358 mg, 50%).  $^1\text{H}$  NMR (400 MHz,  $\text{CDCl}_3$ , 298 K, relative to  $\text{Me}_4\text{Si}$ )/ppm:  $\delta$  = 2.65 (d, 6H;  $-\text{CH}_3$ ), 6.34 (d,  $J$  = 4.0 Hz, 1H; pyrrole proton at 6-position), 6.79 (d,  $J$  = 4.0 Hz, 1H; pyrrole proton at 7-position), 6.85 (s, 1H; pyrrole proton at 1-position), 7.44–7.54 (m, 5H;  $-\text{C}_6\text{H}_5$ ).

**4,4-Difluoro-8-phenyl-2-trimethylsilylethynyl-3,5-dimethyl-4-bora-3a,4a-diaza-*s*-indacene.** To a solution of 4,4-difluoro-8-phenyl-2-iodo-3,5-dimethyl-4-bora-3a,4a-diaza-*s*-indacene (437 mg, 1.04 mmol),  $\text{Pd}(\text{PPh}_3)_4$  (60 mg, 0.05 mmol) and  $\text{CuI}$  (10 mg, 0.05 mmol) in triethylamine (50 mL) was added trimethylsilylacetylene (1.5 mL, 10.4 mmol). The reaction mixture was stirred at room temperature under  $\text{N}_2$  overnight. After evaporation of the solvent, the residue was purified by column chromatography on silica gel using dichloromethane–hexane (1 : 5 v/v) as an eluent to give the product as a red solid (350 mg, 86%).  $^1\text{H}$  NMR (400 MHz,  $\text{CDCl}_3$ , 298 K, relative to  $\text{Me}_4\text{Si}$ )/ppm:  $\delta$  = 0.21 (d, 9H;  $-\text{CH}_3$ ), 2.67 (d, 6H;  $-\text{CH}_3$ ), 6.31 (d,  $J$  = 4.1 Hz, 1H; pyrrole proton at 6-position), 6.77 (d, 2H; pyrrole protons at 1,7-position), 7.46–7.55 (m, 5H;  $-\text{C}_6\text{H}_5$ ).

**4,4-Difluoro-8-phenyl-2-ethynyl-3,5-dimethyl-4-bora-3a,4a-diaza-*s*-indacene.** 4,4-Difluoro-8-phenyl-2-trimethylsilylethynyl-3,5-dimethyl-4-bora-3a,4a-diaza-*s*-indacene (350 mg, 0.89 mmol)

was dissolved in degassed THF (30 mL). Tetra-*n*-butylammonium fluoride (1 mol  $\text{dm}^{-3}$  in THF, 0.9 mL) was injected slowly at  $-78$  °C. The reaction mixture was stirred at  $-78$  °C for 30 min. After evaporation of the solvent, the residue was re-dissolved in dichloromethane (30 mL) and washed with water twice (20 mL  $\times$  2). The organic layer was dried over anhydrous sodium sulfate. Subsequent filtration and removal of the solvent yielded the crude product, which was then purified by flash column chromatography on silica gel using dichloromethane–hexane (1 : 5 v/v) as an eluent to give the pure product (245 mg, 86%).  $^1\text{H}$  NMR (400 MHz,  $\text{CDCl}_3$ , 298 K, relative to  $\text{Me}_4\text{Si}$ )/ppm:  $\delta$  = 2.63–2.73 (d, 6H;  $-\text{CH}_3$ ), 3.18 (s, 1H;  $-\text{C}\equiv\text{CH}$ ), 6.33 (d,  $J$  = 3.8 Hz, 1H; pyrrole proton at 6-position), 6.80 (d, 2H; pyrrole protons at 1,7-position), 7.45–7.54 (m, 5H;  $-\text{C}_6\text{H}_5$ ).

**4:** To a solution of 4,4-difluoro-8-phenyl-2-ethynyl-3,5-dimethyl-4-bora-3a,4a-diaza-*s*-indacene (200 mg, 0.62 mmol),  $[\text{Pd}(\text{PPh}_3)_4]$  (72 mg, 0.06 mmol) and  $\text{CuI}$  (12 mg, 0.063 mmol) in  $\text{Et}_3\text{N}$  (40 mL) was added *p*-iodophenyldimesitylborane (564 mg, 1.25 mmol). The mixture was then heated under reflux for 16 h. After evaporation of the solvent, the residue was purified by column chromatography on silica gel using dichloromethane–hexane (1 : 5 v/v) as an eluent to give **4** as a red solid (171 mg, 42%).  $^1\text{H}$  NMR (400 MHz,  $\text{CDCl}_3$ , 298 K, relative to  $\text{Me}_4\text{Si}$ )/ppm:  $\delta$  = 2.0 (s, 12H;  $-\text{CH}_3$ ), 2.30 (s, 6H;  $-\text{CH}_3$ ), 2.68 (s, 3H;  $-\text{CH}_3$ ), 2.76 (s, 3H;  $-\text{CH}_3$ ), 6.33 (d,  $J$  = 4.2 Hz, 1H; 6-*H*), 6.80 (d,  $J$  = 4.2 Hz, 1H; 7-*H*), 6.82 (s, 4H, mesityl), 6.84 (s, 1H; 1-*H*), 7.42 (d,  $J$  = 8.1 Hz, 2H; mesityl), 7.47 (d,  $J$  = 8.1 Hz, 2H; mesityl), 7.48–7.55 (m, 5H;  $-\text{C}_6\text{H}_5$ ). MS ( $\text{EI}^+$ ):  $m/z$ : 644.77; Anal. Calcd (%) for  $\text{C}_{43}\text{H}_{40}\text{B}_2\text{F}_2\text{N}_2$ : C, 80.14; H, 6.26; N, 4.35; found: C, 79.72; H, 6.32; N, 4.30.

**3-[2-(4-Aza-phenyl-15-crown-5)ethenyl]-4,4-difluoro-8-[4-bromophenyl]-5-methyl-3a,4a-diaza-4-bora-*s*-indacene.** The compound was synthesized by a procedure similar to that used for **1** except that 4,4-difluoro-8-(4-bromophenyl)-3,5-dimethyl-4-bora-3a,4a-diaza-*s*-indacene (1.87 g, 50 mmol) was used instead of 4,4-difluoro-8-(4-hydroxyphenyl)-3,5-dimethyl-4-bora-3a,4a-diaza-*s*-indacene. Yield: 1.32 g, 30%.  $^1\text{H}$  NMR (400 MHz,  $\text{CDCl}_3$ , 298 K, relative to  $\text{Me}_4\text{Si}$ )/ppm:  $\delta$  = 2.66 (s, 3H;  $-\text{CH}_3$ ), 3.60–3.71 (m, 16H;  $-\text{OCH}_2\text{CH}_2\text{N}-$  and  $-\text{OCH}_2\text{CH}_2\text{O}-$ ), 3.80 (t, 4H;  $-\text{OCH}_2\text{CH}_2\text{N}-$ ), 6.25 (d, 1H,  $J$  = 3.9 Hz; pyrrole proton at 2-position), 6.58 (d,  $J$  = 3.9 Hz, 1H; pyrrole proton at 1-position), 6.67 (d,  $J$  = 8.9 Hz, 2H; 5'-*m*-Ar), 6.75 (d,  $J$  = 4.6 Hz, 1H; pyrrole proton at 6-position), 6.90 (d,  $J$  = 4.6 Hz, 1H; pyrrole proton at 7-position), 7.30 (d,  $J$  = 16.1 Hz, 1H; vinyl proton at 5'-position), 7.38 (d,  $J$  = 8.3 Hz, 2H; 8-*o*-Ar), 7.47–7.56 (m, 3H; vinyl proton at 5-position and 5'-*o*-Ar), 7.61 (d,  $J$  = 8.3 Hz, 2H; 8-*m*-Ar).

**3-[2-(4-Aza-phenyl-15-crown-5)ethenyl]-4,4-difluoro-8-[4-trimethylsilylethynylphenyl]-5-methyl-3a,4a-diaza-4-bora-*s*-indacene.** The compound was synthesized by a procedure similar to that used for 4,4-difluoro-8-(4-trimethylsilylethynylphenyl)-3,5-dimethyl-4-bora-3a,4a-diaza-*s*-indacene except that 3-[2-(4-aza-phenyl-15-crown-5)ethenyl]-4,4-difluoro-8-[4-bromophenyl]-5-methyl-3a,4a-diaza-4-bora-*s*-indacene (400 mg, 0.6 mmol) was used. Yield: 360 mg, 86%.  $^1\text{H}$  NMR (400 MHz,  $\text{CDCl}_3$ , 298 K, relative to  $\text{Me}_4\text{Si}$ )/ppm:  $\delta$  = 0.28 (s, 9H;  $-\text{CH}_3$ ), 2.66 (s, 3H;  $-\text{CH}_3$ ), 3.60–3.71 (m, 16H;  $-\text{OCH}_2\text{CH}_2\text{N}-$  and  $-\text{OCH}_2\text{CH}_2\text{O}-$ ),

3.78 (t, 4H;  $-\text{OCH}_2\text{CH}_2\text{N}-$ ), 6.23 (d,  $J = 4.0$  Hz, 1H; pyrrole proton at 2-position), 6.58 (d,  $J = 4.0$  Hz, 1H; pyrrole proton at 1-position), 6.66 (d,  $J = 8.9$  Hz, 2H;  $5'-m\text{-Ar}$ ), 6.74 (d,  $J = 4.6$  Hz, 1H; pyrrole proton at 6-position), 6.89 (d,  $J = 4.6$  Hz, 1H; pyrrole proton at 7-position), 7.29 (d,  $J = 16.1$  Hz, 1H; vinyl proton at  $5'$ -position), 7.42–7.47 (d, 2H;  $5'-o\text{-Ar}$ ), 7.47–7.52 (m, 3H; vinyl proton at 5-position and  $5'-o\text{-Ar}$ ), 7.53–7.59 (d,  $J = 8.3$  Hz, 2H;  $8-m\text{-Ar}$ ).

**3-[2-(4-Aza-phenyl-15-crown-5)ethenyl]-4,4-difluoro-8-[4-ethynyl-phenyl]-5-methyl-3a,4a-diaza-4-bora-s-indacene.** The compound was synthesized by a procedure similar to that used for 4,4-difluoro-8-(4-ethynylphenyl)-3,5-dimethyl-4-bora-3a,4a-diaza-s-indacene except that 3-[2-(4-aza-phenyl-15-crown-5)ethenyl]-4,4-difluoro-8-[4-trimethylsilylethynylphenyl]-5-methyl-3a,4a-diaza-4-bora-s-indacene (287 mg, 0.41 mmol) was used. Yield: 214 mg, 83%.  $^1\text{H}$  NMR (400 MHz,  $\text{CDCl}_3$ , 298 K, relative to  $\text{Me}_4\text{Si}$ )/ppm:  $\delta = 2.66$  (s, 3H;  $-\text{CH}_3$ ), 3.20 (s, 1H;  $-\text{C}\equiv\text{CH}$ ), 3.62–3.70 (m, 16H;  $-\text{OCH}_2\text{CH}_2\text{N}-$  and  $-\text{OCH}_2\text{CH}_2\text{O}-$ ), 3.78 (t, 4H;  $-\text{OCH}_2\text{CH}_2\text{N}-$ ), 6.23 (d,  $J = 4.0$  Hz, 1H; pyrrole proton at 2-position), 6.59 (d,  $J = 4.0$  Hz, 1H; pyrrole proton at 1-position), 6.66 (d,  $J = 8.9$  Hz, 2H;  $5'-m\text{-Ar}$ ), 6.76 (d,  $J = 4.6$  Hz, 1H; pyrrole proton at 6-position), 6.90 (d,  $J = 4.6$  Hz, 1H; pyrrole proton at 7-position), 7.29 (d,  $J = 16.0$  Hz, 1H; vinyl proton at  $5'$ -position), 7.45–7.56 (m, 5H; vinyl proton at 5-position and  $5'-o\text{-Ar}$ ), 7.57–7.61 (d,  $J = 8.3$  Hz, 2H;  $8-m\text{-Ar}$ ).

**5:** The compound was synthesized by a procedure similar to that used for **3** except that 3-[2-(4-aza-phenyl-15-crown-5)ethenyl]-4,4-difluoro-8-[4-ethynylphenyl]-5-methyl-3a,4a-diaza-4-bora-s-indacene (130 mg, 0.21 mmol) was used. Yield: 111 mg, 56%.  $^1\text{H}$  NMR (400 MHz,  $\text{CDCl}_3$ , 298 K, relative to  $\text{Me}_4\text{Si}$ )/ppm:  $\delta = 2.02$  (s, 12H;  $-\text{CH}_3$ ), 2.32 (s, 6H;  $-\text{CH}_3$ ), 2.67 (s, 3H;  $-\text{CH}_3$ ), 3.62–3.72 (m, 16H;  $-\text{OCH}_2\text{CH}_2\text{N}-$  and  $-\text{OCH}_2\text{CH}_2\text{O}-$ ), 3.79 (t, 4H;  $-\text{OCH}_2\text{CH}_2\text{N}-$ ), 6.24 (d,  $J = 3.9$  Hz, 2H; pyrrole proton at 2-position), 6.63 (d,  $J = 3.9$  Hz, 1H; pyrrole proton at 1-position), 6.67 (d,  $J = 8.9$  Hz, 2H;  $5'-m\text{-Ar}$ ), 6.80 (d,  $J = 4.6$  Hz, 2H; pyrrole proton at 6-position), 6.84 (s, 4H; mesityl), 6.91 (d,  $J = 4.6$  Hz, 1H; pyrrole proton at 7-position), 7.30 (d,  $J = 16.0$  Hz, 1H; vinyl proton at  $5'$ -position), 7.45–7.57 (m, 9H; vinyl proton at  $5'$ -position and Ar), 7.64 (d,  $J = 8.2$  Hz, 2H; Ar). MS ( $\text{EI}^+$ ):  $m/z$ : 949.79; Anal. Calcd (%) for  $\text{C}_{60}\text{H}_{63}\text{B}_2\text{F}_2\text{N}_3\text{O}_4$ : C, 75.87; H, 6.69; N, 4.42; found: C, 75.87; H, 6.68; N, 4.42.

### Physical measurements and instrumentation

$^1\text{H}$  NMR spectra were recorded on a Bruker DPX-400 (400 MHz) or a Bruker DPX-500 (500 MHz) FT-NMR spectrometer in  $\text{CDCl}_3$  at 298 K and chemical shifts ( $\delta$ , ppm) were reported relative to tetramethylsilane ( $\text{Me}_4\text{Si}$ ). Elemental analyses of the compounds were performed on a Flash EA 1112 elemental analyzer at the Changchun Institute of Applied Chemistry, Chinese Academy of Sciences. EI mass spectra were recorded on a Thermo Scientific ITQ 1100<sup>TM</sup> GC/MSn. Positive-ion electrospray-ionization (ESI) mass spectra were obtained on a Finnigan LCQ mass spectrometer. MALDI-TOF MS was performed on an Autoflex speed TOF/TOF mass spectrometer (Bruker Daltonics, Leipzig, Germany). Electronic absorption spectra were obtained using a Varian Cary 50 UV-vis

spectrophotometer, while the emission titration was performed on a Horiba Jobin Yvon Fluorolog-3 Spectrofluorometer. For the determination of the emission quantum yields  $\Phi$  in  $\text{CH}_3\text{CN}$ , quinine sulphate in 1 N  $\text{H}_2\text{SO}_4$  ( $\Phi = 0.546$ ) was used as the reference standard.<sup>17</sup>

The concentrations of **1** and **2** employed in the UV-vis and emission titration studies were typically fixed at  $1.0 \times 10^{-5}$  mol  $\text{dm}^{-3}$ . The electronic absorption spectral titration was performed on a Varian Cary 50 UV-vis spectrophotometer at room temperature, while the emission titration was performed on a Horiba Jobin Yvon Fluorolog-3 Spectrofluorometer. Supporting electrolyte (0.1 M  $n\text{Bu}_4\text{NClO}_4$ ) was added to maintain a constant ionic strength of the sample solution. The  $\text{pK}_a$  values of the amino group on the azacrown and the phenolic group are found based on eqn (1).<sup>18</sup>

$$\log[(A_{\max} - A)/(A - A_{\min})] = \text{pH} - \text{pK}_a \quad (1)$$

Based on eqn (1), a plot of  $\log[(A_{\max} - A)/(A - A_{\min})]$  against pH gave a straight line with a y-intercept, which equals  $\text{pK}_a$ .

Binding constants for 1 : 1 complexation were obtained by a nonlinear least-squares fit<sup>19</sup> of the absorbance ( $A$ ) or emission intensity ( $I$ ) versus the concentration of the ions added ( $C_m$ ) according to the following equation:

$$A = A_0 + \frac{A_{\text{lim}} - A_0}{2C_0} \{C_0 + C_m + 1/K_s - [(C_0 + C_m + 1/K_s)^2 - 4C_0C_m]^{1/2}\} \quad (2)$$

where  $A_0$  and  $A$  are the absorbance of the complex at a selected wavelength in the absence and presence of the metal cations, respectively,  $C_0$  is the total concentration of the BODIPY-containing azacrown,  $C_m$  is the concentration of the added ions,  $A_{\text{lim}}$  is the limiting value of absorbance at saturation level, and  $K_s$  is the stability constant. For emission titration studies, eqn (2) can be modified to give eqn (3), written as

$$I = I_0 + \frac{I_{\text{lim}} - I_0}{2C_0} \{C_0 + C_m + 1/K_s - [(C_0 + C_m + 1/K_s)^2 - 4C_0C_m]^{1/2}\} \quad (3)$$

where  $I_0$  and  $I$  are the emission intensity of the BODIPY compounds at a selected wavelength in the absence and presence of ions, respectively, and  $I_{\text{lim}}$  is the limiting value of emission intensity at saturation level.

Single crystals of **1** suitable for X-ray diffraction studies were grown by the layering of  $n$ -hexane onto a dichloromethane solution of the complex. The single-crystal X-ray diffraction data for compound **1** were collected on a Rigaku R-Axis RAPID imaging plate diffractometer with graphite-monochromated  $\text{Mo-K}\alpha$  ( $\lambda = 0.71073$  Å). The structure was solved by direct methods employing the SHELXS-97 program.<sup>20</sup> Full-matrix least-squares refinement on  $F^2$  was used in the structure refinement. The positions of H atoms were calculated based on riding mode with thermal parameters equal to 1.2 times that of the associated C atoms and participated in the calculation of final  $R$ -indices. In the final stage of least-squares refinement, all non-hydrogen atoms were refined anisotropically. Crystallography and structural refinement data are given in Table S1.†

CCDC-867744 (**1**) contains the supplementary crystallographic data for this paper.

## Results and discussion

### X-ray crystal structure

Fig. S1a† shows the perspective view of the molecular structure of **1** showing a tetrahedral  $\text{BF}_2\text{N}_2$  geometry. The selected bond lengths and angles are listed in Table S2.† The bond lengths for B–N and B–F and the N–B–N and F–B–F bond angles are in good agreement with previously reported data.<sup>21</sup> The shorter bond length of 1.330(3) Å for C(17)–C(18) in the crystal structure indicates that C(17)–C(18) is a double bond in *trans* geometry formed by the condensation reaction between 4,4-difluoro-3,5-dimethyl-8-(4-hydroxyphenyl)-4-bora-3a,4a-diaza-*s*-indacene and 4-formyl-*N*-phenylaza-15-crown-5. Similar to other BODIPY derivatives,<sup>21b,c</sup> the phenyl and indacene planes are approximately perpendicular to each other with a dihedral angle of 76.17°, resulting from the steric hindrance between the 1,7-hydrogen atoms at the 1,7-positions on the indacene moiety and the hydrogen atom at the 8-position of the *meso*-phenyl moiety. The dihedral angle of 18.70° between indacene and the styryl group suggests the less effective conjugation within the entire chromophore. Although there are no  $\pi$ – $\pi$  stacking interactions, a dimeric arrangement is observed between two adjacent molecules with intermolecular hydrogen bonds (Fig. S1b†). A short

contact distance of 1.97 Å between the hydroxy group and the azacrown unit is observed.

### Solvent-dependent UV-vis absorption and emission studies

The electronic absorption spectra of **1** in various solvents at 298 K show intense absorption bands at 619–631 nm and moderately intense bands at 350–500 nm. The electronic absorption spectra of **1** in several solvents are shown in Fig. 1a, and the photophysical data in different solvents are listed in Table 1. With reference to previous work on *p*-aminostyryl-linked BODIPY derivatives,<sup>16</sup> the absorption bands at 380–450 nm with molar extinction coefficients in the order of  $10^4 \text{ dm}^3 \text{ mol}^{-1} \text{ cm}^{-1}$  in the high-energy absorption band are assigned to the  $\text{S}_0 \rightarrow \text{S}_2$  and  $\text{S}_0 \rightarrow \text{S}_3$  transitions. The intense low-energy absorption bands with molar extinction coefficients in the order of  $10^5 \text{ dm}^3 \text{ mol}^{-1} \text{ cm}^{-1}$  at about 619–631 nm are assigned to the 0 → 0 vibrational band of the strong  $\text{S}_0 \rightarrow \text{S}_1$  transition of **1** with some charge-transfer character from the azacrown moiety to the BODIPY moiety, as supported by the slight sensitivity towards solvent polarity (Fig. 1a). A shoulder at approximately 585 nm is assigned to the  $\text{S}_0 \rightarrow \text{S}_1$  vibrational band of the same transition.

In contrast, the emission energy of **1** is found to be sensitive to the solvent polarity. This assignment with charge transfer character is supported by its sensitivity towards solvent polarity. Upon increasing the solvent polarity from chloroform to DMF,

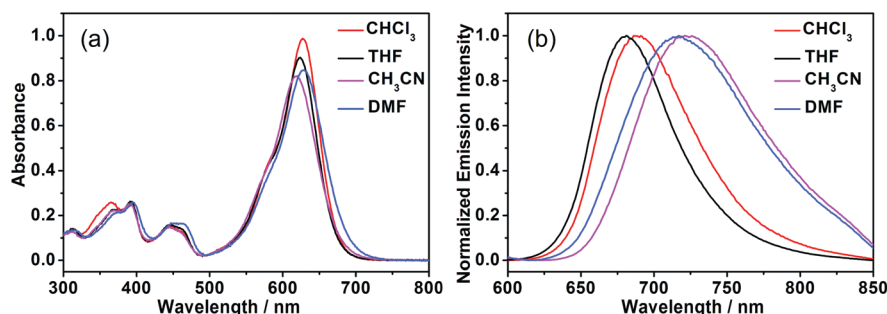


Fig. 1 (a) UV-vis absorption spectra and (b) normalized emission spectra of **1** in selected solvents at 298 K.

Table 1 Summary for electronic absorption and emission energies for **1** in various solvents

Solvent	$\lambda_{\text{abs}}/\text{nm}$	$\lambda_{\text{em}}/\text{nm}$	$\Delta\bar{\nu}/\text{cm}^{-1}$	Refractive index ( $n$ )	Dielectric constant ( $\epsilon$ )	$\Delta f^a$
Ethyl acetate	619	680	1449	1.37	6.1	0.20
Acetone	619	707	2011	1.36	20.7	0.28
Acetonitrile	619	717	2234	1.34	35.9	0.30
1-Butanol	620	686	1552	1.40	17.5	0.26
Chloroform	627	681	1265	1.45	4.8	0.15
Dichloromethane	626	700	1689	1.42	8.9	0.22
Diethyl ether	616	666	1219	1.35	4.3	0.17
DMF	629	723	2067	1.43	36.7	0.28
DMSO	634	729	2055	1.48	46.5	0.26
Ethanol	618	694	1722	1.36	24.6	0.29
Methanol	616	699	1928	1.33	32.7	0.31
1-Propanol	620	690	1636	1.39	20.45	0.28
2-Propanol	617	677	1436	1.38	19.92	0.28
THF	623	690	1559	1.41	7.58	0.21

$$^a \Delta f = f(\epsilon) - f(n^2) = \frac{\epsilon-1}{2\epsilon+1} - \frac{n^2-1}{2n^2+1}$$

a significant red shift with  $\Delta E_{em}$  of *ca.* 1030  $\text{cm}^{-1}$  is observed (Fig. 1b). This indicates that this structureless emission band originates from an intramolecular charge transfer (ICT) excited state due to the presence of the electron-donating nitrogen atom of the azacrown.<sup>16,22b</sup> The emission energies are found to shift to the red with an increase in the dielectric constant of the solvent from chloroform to DMF:  $\text{CHCl}_3$  (681 nm) > THF (691 nm) > MeCN (719 nm) > DMF (722 nm). This may be attributed to the significant increase in the dipole moment of the excited state, which is stabilized in a polar solvent medium, relative to its ground state. It is found that the Stokes shift is well correlated with the Lippert solvent parameter (Fig. 2).<sup>23</sup>

### Acid–base titration studies

Compound **1** exhibits drastic color changes from blue to yellow in acetonitrile upon addition of  $\text{HClO}_4$ . Upon increasing the acid concentration, the electronic absorption spectra of **1** show a drop in the absorbance of the lowest energy absorption band at 619 nm with a growth of the higher energy absorption band at 561 nm. Two well-defined isosbestic points at 478 and 575 nm are observed, indicating a clean conversion of **1** to its protonated form.<sup>22,24</sup> The UV-vis spectral traces are shown in Fig. 3a. The drastic color changes are ascribed to the protonation of the tertiary amino group in **1**, in which the electron-donating ability of the tertiary amino group is decreased, leading to a blue shift in transition energy as a result of the decrease in the charge transfer character.

The corresponding emission spectroscopic study has also been investigated. A dramatic emission enhancement at 576 nm has

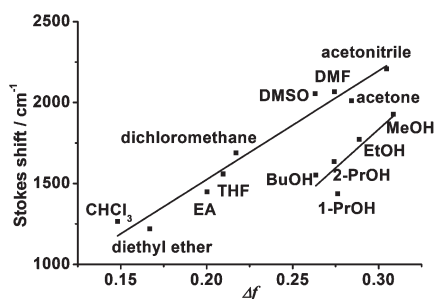


**Fig. 2** Plot of the Stokes shifts  $\Delta\bar{\nu}$  (in  $\text{cm}^{-1}$ ) of **1** in various solvents against the Lippert solvent parameter  $\Delta f$  ( $\Delta f = f(\epsilon) - f(n^2)$ ).

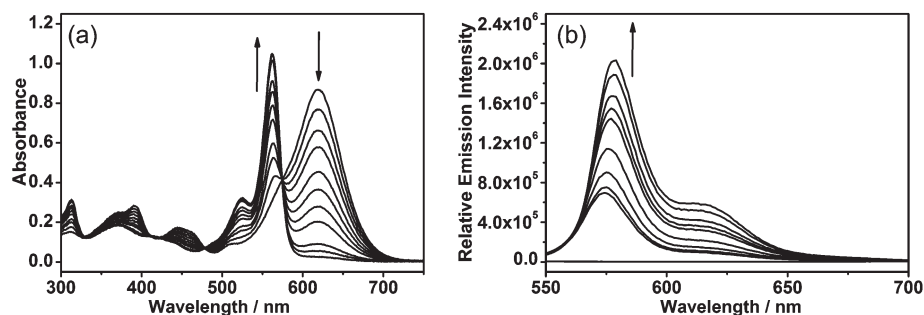


**Fig. 3** (a) UV-vis absorption spectral changes of **1** (concentration =  $10^{-5}$  mol  $\text{dm}^{-3}$ ) in acetonitrile (0.1 M  ${}^n\text{Bu}_4\text{NClO}_4$ ) upon addition of  $\text{HClO}_4$ . (b) Emission spectral changes of **1** (concentration =  $10^{-5}$  mol  $\text{dm}^{-3}$ ) in acetonitrile (0.1 M  ${}^n\text{Bu}_4\text{NClO}_4$ ) upon addition of  $\text{HClO}_4$ .

been observed with increasing  $\text{HClO}_4$  concentration in acetonitrile at room temperature. The observation of the weak BODIPY emission ( $\Phi = 0.018$ ) in **1** before protonation is due to a photoinduced electron transfer (PET) quenching pathway from the amino group. The revival of the vibronic-structured emission band together with significant emission enhancement ( $\Phi = 0.541$  after protonation) is ascribed to the elimination of the PET quenching pathway as a result of the decrease of the electron-donating ability upon protonation of the amino group of **1**. The emission spectral changes of **1** are shown in Fig. 3b.

Upon the addition of  ${}^n\text{Bu}_4\text{NOH}$ , the lowest energy absorption band at 619 nm is found to shift to 646 nm, while the absorption band at 550 nm shows a drop in absorbance. Two well-defined isosbestic points at 565 and 640 nm are observed (Fig. 4a). Such a bathochromic shift is attributed to the better  $\pi$ -conjugation between the phenolate and the BODIPY moieties upon deprotonation of the hydroxy group. Upon excitation at the isosbestic wavelength at 477 nm, the emission intensity decreases ( $\Phi = 0.007$ ) upon addition of  ${}^n\text{Bu}_4\text{NOH}$  due to enhanced PET quenching exerted by the anionic phenolate moiety (Fig. 4b). The  $\text{pK}_a$  value has been determined by studying under different pH conditions. The  $\text{pK}_a$  values of the amino group on the azacrown and the phenolic group are found to be 2.0 and 8.99, respectively, from the inflection point of the plot of  $\log[(A_{\text{max}} - A)/(A - A_{\text{min}})]$  against pH (Fig. 5).

### Cation-binding properties

The cation-binding properties of **1** with alkali metal ions ( $\text{Li}^+$  and  $\text{Na}^+$ ), alkaline earth metal ions ( $\text{Mg}^{2+}$  and  $\text{Ba}^{2+}$ ) and transition metal ions ( $\text{Zn}^{2+}$  and  $\text{Cd}^{2+}$ ) have been investigated by the electronic absorption spectrophotometric method. Upon addition of monovalent  $\text{Li}^+$  and  $\text{Na}^+$  to an acetonitrile solution of **1** (0.1 M  ${}^n\text{Bu}_4\text{NClO}_4$ ), the  $S_0 \rightarrow S_1$  transition band shows a slight blue shift in energy. In contrast, addition of divalent alkaline earth metal ions ( $\text{Mg}^{2+}$  and  $\text{Ba}^{2+}$ ) and transition metal ions ( $\text{Zn}^{2+}$  and  $\text{Cd}^{2+}$ ) to **1** gives drastic color changes from purple to pink together with dramatic UV-vis absorption spectral changes, in which the  $S_0 \rightarrow S_1$  transition band shows a significant blue shift in energy from *ca.* 619 to *ca.* 567 nm with well-defined isosbestic points at *ca.* 484 and 583 nm. Fig. 6a and 7a show the UV-vis absorption spectral changes of **1** in acetonitrile solution (0.1 M  ${}^n\text{Bu}_4\text{NClO}_4$ ) upon addition of  $\text{Mg}^{2+}$  and  $\text{Zn}^{2+}$  ions,

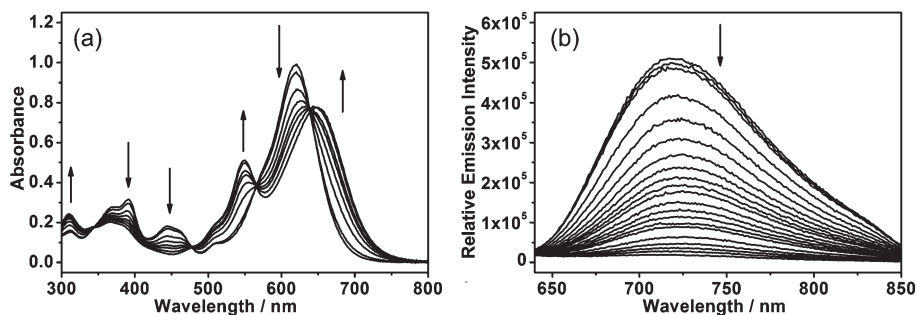


**Fig. 4** (a) UV-vis absorption spectral changes of **1** (concentration =  $10^{-5}$  mol dm $^{-3}$ ) in acetonitrile (0.1 M  $t\text{Bu}_4\text{NClO}_4$ ) upon addition of  $t\text{Bu}_4\text{NOH}$ . (b) Emission spectral changes of **1** (concentration =  $10^{-5}$  mol dm $^{-3}$ ) in acetonitrile (0.1 M  $t\text{Bu}_4\text{NClO}_4$ ) upon addition of  $t\text{Bu}_4\text{NOH}$ .

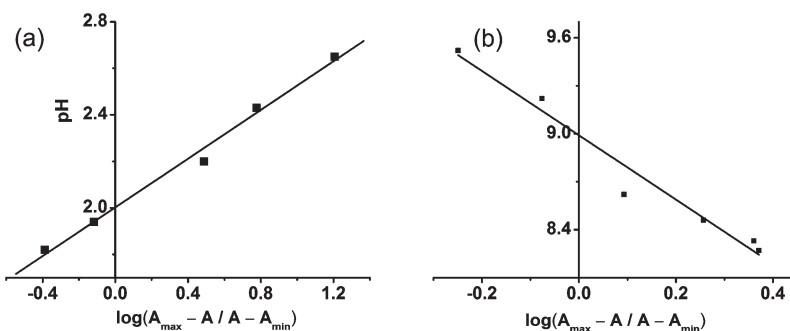


**Fig. 5** A plot of pH vs.  $\log[(A_{\max} - A)/(A - A_{\min})]$  monitored at  $\lambda = 619$  nm (■) and its linear fit (—) for **1**.

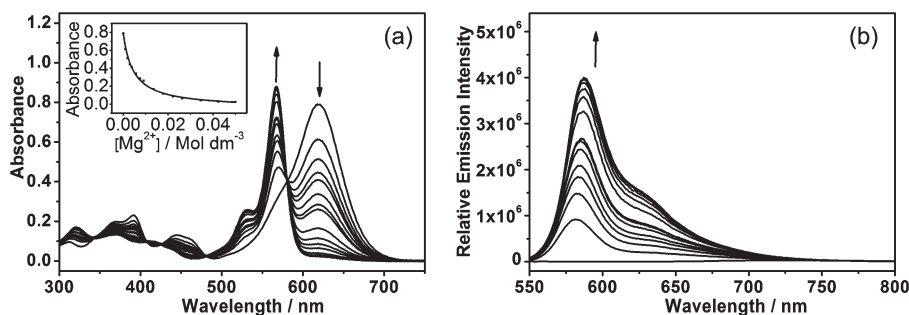


**Fig. 6** (a) UV-vis absorption spectral changes of **1** (concentration =  $10^{-5}$  mol dm $^{-3}$ ) in acetonitrile (0.1 M  $t\text{Bu}_4\text{NClO}_4$ ) upon addition of  $\text{Mg}(\text{ClO}_4)_2$ . The insert shows a plot of absorbance vs.  $[\text{Mg}^{2+}]$  monitored at  $\lambda = 619$  nm and its theoretical fit (—). (b) Emission spectral changes of **1** (concentration =  $10^{-5}$  mol dm $^{-3}$ ) in acetonitrile (0.1 M  $t\text{Bu}_4\text{NClO}_4$ ) upon addition of  $\text{Mg}(\text{ClO}_4)_2$ .

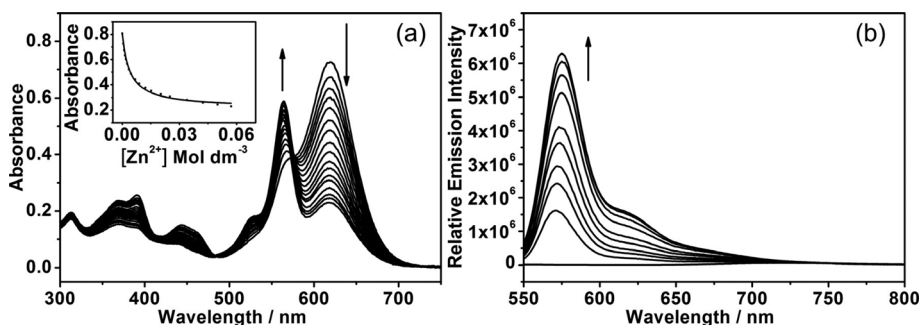


**Fig. 7** (a) UV-vis absorption spectral changes of **1** (concentration =  $10^{-5}$  mol dm $^{-3}$ ) in acetonitrile (0.1 M  $t\text{Bu}_4\text{NClO}_4$ ) upon addition of  $\text{Zn}(\text{ClO}_4)_2$ . The insert shows a plot of absorbance vs.  $[\text{Zn}^{2+}]$  monitored at  $\lambda = 619$  nm and its theoretical fit (—). (b) Emission spectral changes of **1** (concentration =  $10^{-5}$  mol dm $^{-3}$ ) in acetonitrile (0.1 M  $t\text{Bu}_4\text{NClO}_4$ ) upon addition of  $\text{Zn}(\text{ClO}_4)_2$ .

respectively. The experimental data show a nice agreement with the theoretical fits (inserts of Fig. 6a and 7a). The identity of the 1 : 1  $\text{Mg}^{2+}$ -**1** adduct has further been supported by positive-ion ESI-MS experiments (Fig. S2†). The binding constants ( $\log K_s$ ) of **1** with various metal ions in acetonitrile have been determined and summarized in Table 2. Similar to the addition of acid, various metal ions encapsulated in the cavity of the azacrown would lower the electron-donating ability of the amino group, leading to an increase in the HOMO-LUMO gap. In general, **1** shows more drastic UV-vis absorption spectral changes towards divalent metal ions. This can be attributed to the higher binding affinity as well as the higher charge density of the divalent metal ions which would render the amino group more electron-deficient.

Compound **2** with two azacrown moieties also exhibits interesting cation-binding behaviors. Upon addition of  $\text{Mg}^{2+}$  and  $\text{Zn}^{2+}$ , the  $S_0 \rightarrow S_1$  transition band shows a significant blue shift

**Table 2** Stability constants of **1** for various metal ions in acetonitrile (0.1 M  $n\text{Bu}_4\text{NClO}_4$ ) at 298 K by the UV-visible spectrophotometric method

Metal ions added	$\log K_s$
$\text{LiClO}_4$	$2.44 \pm 0.03$
$\text{NaClO}_4$	$2.02 \pm 0.02$
$\text{Mg}(\text{ClO}_4)_2$	$2.32 \pm 0.02$
$\text{Ba}(\text{ClO}_4)_2$	$3.10 \pm 0.01$
$\text{Zn}(\text{ClO}_4)_2$	$2.39 \pm 0.01$
$\text{Cd}(\text{ClO}_4)_2$	$2.82 \pm 0.01$

in energy (Fig. 8a and 9a). In contrast to **1**, no well-defined isosbestic points are observed in the UV-vis spectral profile. This is possibly attributed to the occurrence of two binding processes with stoichiometries of both 2 : 1 and 1 : 1. The 2 : 1 binding mode has also been supported by the positive-ion ESI and MALDI-TOF mass spectral studies of **2** upon addition of  $\text{Mg}^{2+}$ , which showed an ion cluster at  $m/z$  484 corresponding to the  $[\text{2}\cdot\text{2Mg} - 2\text{H}]^+$  adduct (Fig. S3†) and an ion cluster at  $m/z$  1269 corresponding to the  $[\text{2}\cdot\text{2Mg}\cdot\text{3ClO}_4]^+$  adduct (Fig. S4†), respectively. Also, the Hill plot suggests that the interaction of **2** with  $\text{Mg}^{2+}$  is cooperative, as revealed by a Hill coefficient of 1.90 with an overall binding constant ( $\log K$ ) of 3.55. On the other hand, binding of  $\text{Zn}^{2+}$  gives a Hill coefficient of 1.05, suggesting that the two  $\text{Zn}^{2+}$  binding processes are completely independent of each other.

The emission studies upon addition of metal ions have also been studied in acetonitrile solutions of **1**. Upon the addition of monovalent metal ions, such as  $\text{Li}^+$  and  $\text{Na}^+$ , a slight increase in emission intensity is observed due to the small binding affinity of the azacrown for the monovalent metal ions. In contrast, addition of divalent metal ions leads to significant emission enhancement of a vibronic-structured band at *ca.* 580 nm upon excitation at the isosbestic wavelength. Fig. 6b and 7b show the emission spectral changes upon addition of  $\text{Mg}^{2+}$  and  $\text{Zn}^{2+}$ . Similarly, **2** shows dramatic emission enhancement upon addition of  $\text{Mg}^{2+}$  (Fig. 8b) and  $\text{Zn}^{2+}$  (Fig. 9b). The photoluminescence quantum yields of the complex have been determined and summarized in Table 3. The observation of emission enhancement in **1** and **2** upon addition of divalent metal ions can

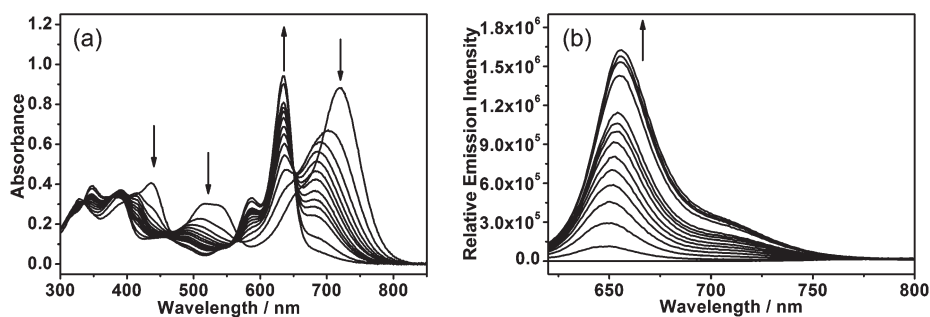


**Fig. 8** (a) UV-vis absorption spectral changes of **2** (concentration =  $10^{-5}$  mol  $\text{dm}^{-3}$ ) in acetonitrile (0.1 M  $n\text{Bu}_4\text{NClO}_4$ ) upon addition of  $\text{Mg}(\text{ClO}_4)_2$ . (b) Emission spectral changes of **2** (concentration =  $10^{-5}$  mol  $\text{dm}^{-3}$ ) in acetonitrile (0.1 M  $n\text{Bu}_4\text{NClO}_4$ ) upon addition of  $\text{Mg}(\text{ClO}_4)_2$ .

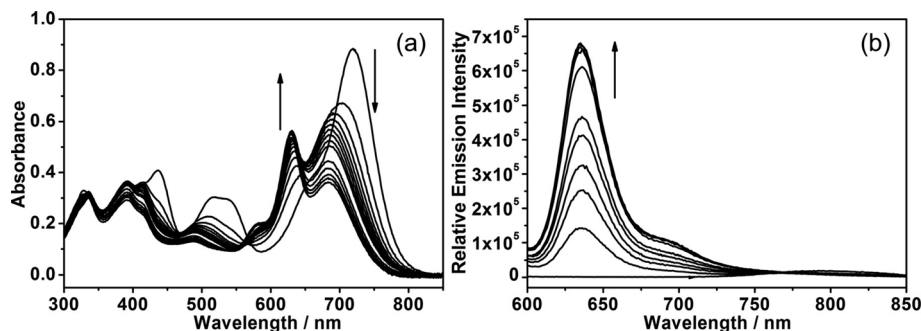


**Fig. 9** (a) UV-vis absorption spectral changes of **2** (concentration =  $10^{-5}$  mol  $\text{dm}^{-3}$ ) in acetonitrile (0.1 M  $n\text{Bu}_4\text{NClO}_4$ ) upon addition of  $\text{Zn}(\text{ClO}_4)_2$ . (b) Emission spectral changes of **2** (concentration =  $10^{-5}$  mol  $\text{dm}^{-3}$ ) in acetonitrile (0.1 M  $n\text{Bu}_4\text{NClO}_4$ ) upon addition of  $\text{Zn}(\text{ClO}_4)_2$ .

be ascribed to the blocking of the intramolecular PET quenching process induced by the encapsulation of the cation by the azacrown moiety, as a result of the decrease in the electron-donating ability of the amino group (Fig. 10). Alternatively, coordination of divalent metal ions would cause an increase in rigidity of the molecule, resulting in less efficient relaxation of the excited state to ground state *via* non-radiative processes. As a result, the

lowest energy emissive excited state is changed from the ICT to the  $S_0 \rightarrow S_1$  excited state that emits at higher energy.

### Fluoride-binding properties

It is known that triarylborane is a selective and sensitive moiety for fluoride ion-binding by utilization of the empty  $p_\pi$  orbital on the boron center to form four-coordinate triarylfluoroborate compounds. BODIPY derivatives **3** and **4** with dimesitylboron moieties were synthesized to study the fluoride ion-binding properties. Interestingly, **3** and **4** show different electronic spectral changes towards fluoride ions in acetonitrile solution (0.1 M  ${}^n\text{Bu}_4\text{NClO}_4$ ). Upon addition of fluoride ions to **3**, the absorption band at 335 nm diminishes in intensity with the growth of an absorption band at 260 nm with small perturbation of the low-energy BODIPY absorption, which is mainly located at 511 nm (Fig. 11a). In contrast, **4** with a triarylborane moiety at the 2-position of the BODIPY skeleton shows the growth of a new absorption tail at 592 nm with a diminution of the absorption band at 548 nm, which is assigned as the  $S_0 \rightarrow S_1$  transition band of the BODIPY chromophore (Fig. 11b). A drastic coloration change is also observed from mauve to purple. The

**Table 3** The emission quantum yields of compound **1–5** and their ion-bound adduct

Complex	$\Phi$	Complex	$\Phi$
<b>1</b>	0.018	<b>2</b>	0.025
<b>1–H<sup>+</sup></b>	0.541	<b>2–Mg<sup>2+</sup></b>	0.469
<b>1–Li<sup>+</sup></b>	0.055	<b>2–Zn<sup>2+</sup></b>	0.094
<b>1–Na<sup>+</sup></b>	0.033	<b>3</b>	0.017
<b>1–Mg<sup>2+</sup></b>	0.476	<b>3–F<sup>-</sup></b>	0.007
<b>1–Ba<sup>2+</sup></b>	0.078	<b>4</b>	0.227
<b>1–Zn<sup>2+</sup></b>	0.031	<b>4–F<sup>-</sup></b>	0.009
<b>1–Cd<sup>2+</sup></b>	0.255	<b>5</b>	0.007
<b>1–OH<sup>-</sup></b>	0.007	<b>5–Mg<sup>2+</sup></b>	0.171
		<b>5–F<sup>-</sup></b>	0.006
		<b>5–F<sup>-</sup>–Mg<sup>2+</sup></b>	0.169

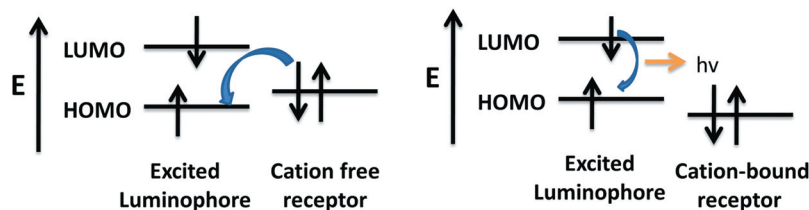


**Fig. 10** Molecular orbital energy diagrams which show the relative energetic dispositions of the frontier orbitals of the fluorophore and the receptor in (left) the analyte-free situation and (right) the analyte-bound situation.

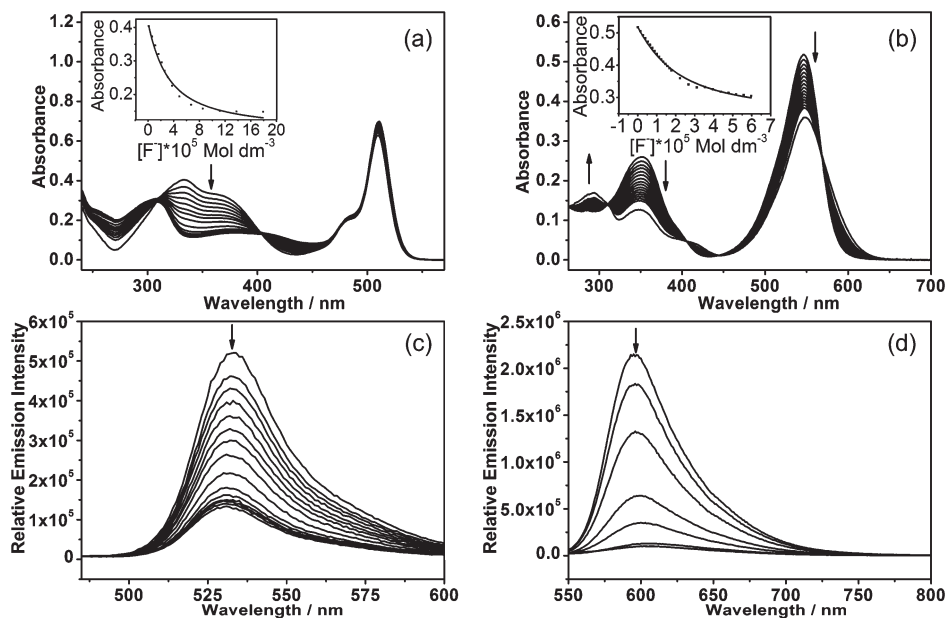


**Fig. 11** UV-vis absorption spectral changes of (a) **3** and (b) **4** (concentration =  $10^{-5}$  mol  $\text{dm}^{-3}$ ) in acetonitrile (0.1 M  ${}^n\text{Bu}_4\text{NClO}_4$ ) upon addition of  ${}^n\text{Bu}_4\text{NF}$ . The inserts show the corresponding plot of absorbance against  $[\text{F}^-]$  monitored at  $\lambda =$  (a) 333 nm and (b) 542 nm and their theoretical fits (—). Emission spectral changes of (c) **3** and (d) **4** (concentration =  $10^{-5}$  mol  $\text{dm}^{-3}$ ) in acetonitrile (0.1 M  ${}^n\text{Bu}_4\text{NClO}_4$ ) upon addition of  ${}^n\text{Bu}_4\text{NF}$ .

difference in the spectral observation of **3** and **4** in response to fluoride ions is attributed to the different degree of perturbation on the BODIPY excited state. In compound **3**, the introduction of the triarylborane moiety at the *meso* position has negligible effect on the BODIPY excited state due to the large dihedral angle between the planes of the dimethylborylphenylethynylphenyl ( $\text{Mes}_2\text{BC}_6\text{H}_4\text{C}\equiv\text{CC}_6\text{H}_4$ ) moiety and the indacene, as revealed by the X-ray crystal structure of **1**. This leads to less effective  $\pi$ -conjugation between the triarylborane and the BODIPY moieties. In contrast, the triarylborane in **4** shows more effective  $\pi$ -conjugation with BODIPY since the presence of the ethynyl spacer minimizes steric repulsion between these two moieties. As a result,  $\text{F}^-$  complexation can influence the BODIPY excited state by enhancement of the ICT character since the triarylfluoroborate is a better donor than triarylborane. This leads to the appearance of a new low-energy absorption tail. Upon excitation at the isosbestic wavelengths, both compounds show emission diminution (**3**:  $\Phi = 0.017 \rightarrow 0.007$ ; **4**:  $\Phi = 0.227 \rightarrow 0.009$ ) due to the enhanced photoinduced electron transfer upon fluoride ion complexation (Fig. 11c and d).

### Ditopic binding properties

The ditopic binding properties of **5** with azacrown and triarylborane moieties have been investigated. Similar to that of **1**, **5** could form a 1 : 1 adduct in the presence of  $\text{Mg}^{2+}$ . This has been supported by the positive-ion ESI mass spectral studies of **5** upon addition of  $\text{Mg}^{2+}$ , which showed an ion cluster at  $m/z$  972.5 corresponding to the  $[\text{5} \cdot \text{Mg} - \text{H}]^+$  adduct (Fig. S5†). Addition of both  $\text{Mg}^{2+}$  and  $\text{F}^-$  also gives significant emission enhancement (Fig. 12). On the basis of the  $\text{Mg}^{2+}$  and  $\text{F}^-$  binding studies in **1** and **3** respectively, in which both binding processes are known to have opposite effect on the emission properties in that  $\text{Mg}^{2+}$  binding gives emission enhancement while  $\text{F}^-$  binding gives emission diminution, the net increase in emission intensity upon ditopic binding suggests that photoinduced electron transfer quenching arising from the addition of  $\text{F}^-$  cannot substantially suppress the emission enhancement arising from the addition of  $\text{Mg}^{2+}$ . This can be supported by the observation that **5** with excess  $\text{Mg}^{2+}$  showed negligible emission diminution ( $\Phi = 0.171 \rightarrow 0.169$ ) even upon addition of  $\text{F}^-$  (Fig. 12).

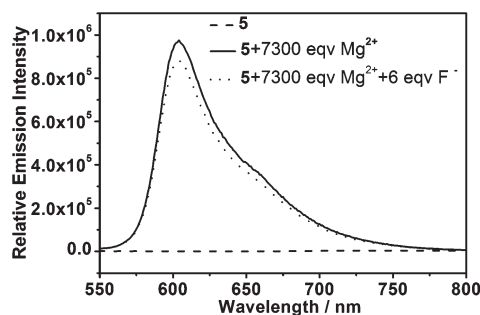


**Fig. 12** Emission spectral changes of **5** upon subsequent addition of  $\text{Mg}(\text{ClO}_4)_2$  and  $t\text{Bu}_4\text{NF}$  in acetonitrile (0.1 M  $t\text{Bu}_4\text{NClO}_4$ ).

### Conclusion

A series of BODIPY derivatives containing ion- and pH-sensory units have been successfully synthesized and characterized. One of the compounds has been structurally characterized by X-ray crystallography, in which the existence of intermolecular hydrogen bonding between the hydroxy group and the azacrown moiety leads to a dimeric structure. Owing to the presence of ICT absorption, **1** showed a structureless ICT emission band in acetonitrile solutions that is found to be highly sensitive towards solvent polarity. Due to the presence of the hydroxy group and the azacrown moiety in compound **1**, its electronic absorption and emission properties are found to be sensitive towards acid, base and divalent cations by perturbation of its ICT excited state. Compound **2** with two azacrown moieties forms 1 : 2 adducts with  $\text{Mg}^{2+}$  and  $\text{Zn}^{2+}$ . The fluoride ion-binding properties of **3** and **4** were also studied. It was found that incorporation of the triarylborane moiety would lead to different electronic absorption spectral changes. Ditopic binding study of **5**, which was functionalized with both azacrown and triarylborane moieties, showed emission enhancement in the presence of  $\text{Mg}^{2+}$  and  $\text{F}^-$ . These findings suggest that these BODIPY derivatives are capable of serving as versatile colorimetric and luminescence probes for pH, cations and  $\text{F}^-$ .

### Acknowledgements

V.W.-W.Y. acknowledges support from The University of Hong Kong and Jilin University. We also acknowledge support from the State Key Laboratory of Supramolecular Structure and Materials in Jilin University and the University Grants Committee Areas of Excellence Scheme (AoE/P-03/08). A.Y.-Y.T. acknowledges the receipt of a University Postdoctoral Fellowship, and C.-T.P. the receipt of a Postgraduate Studentship, both from The University of Hong Kong. Dr H.-L. Wong and Mr F. K.-W. Hau are thanked for their help in ESI-MS measurement. Ms L. Wang is thanked for her help in MALDI-TOF MS measurement.

### References

- (a) R. M. Izatt, J. S. Bradshaw, S. A. Nielsen, J. D. Lamb and J. J. Christensen, *Chem. Rev.*, 1985, **85**, 271; (b) R. M. Izatt, J. S. Bradshaw and R. L. Bruening, *Chem. Rev.*, 1991, **91**, 1721; (c) J. C. Ma and D. A. Dougherty, *Chem. Rev.*, 1997, **97**, 1303; (d) K. A. Connors, *Chem. Rev.*, 1997, **97**, 1325; (e) F. P. Schmidtchen and M. Berger, *Chem. Rev.*, 1997, **97**, 1609; (f) M. M. Conn and J. Rebeck, *Chem. Rev.*, 1997, **97**, 1647; (g) F. Zeng and S. C. Zimmermann, *Chem. Rev.*, 1997, **97**, 1681; (h) A. Ikeda and S. Shinkai, *Chem. Rev.*, 1997, **97**, 1713; (i) V. W. W. Yam and K. K. W. Lo, *Coord. Chem. Rev.*, 1999, **184**, 157; (j) X. M. He and V. W. W. Yam, *Coord. Chem. Rev.*, 2011, **255**, 2111.
- (a) V. W. W. Yam, R. P. L. Tang, K. M. C. Wong, C. C. Ko and K. K. Cheung, *Inorg. Chem.*, 2001, **40**, 571; (b) V. W. W. Yam, R. P. L. Tang, K. M. C. Wong and K. K. Cheung, *Organometallics*, 2001, **20**, 4476; (c) V. W. W. Yam, R. P. L. Tang, K. M. C. Wong, X. X. Lu, K. K. Cheung and N. Y. Zhu, *Chem.-Eur. J.*, 2002, **8**, 4066.
- (a) V. W. W. Yam, Y. L. Pui, K. K. Cheung and N. Y. Zhu, *New J. Chem.*, 2002, **26**, 536; (b) W. S. Tang, X. X. Lu, K. M. C. Wong and V. W. W. Yam, *J. Mater. Chem.*, 2005, **15**, 2714; (c) M. J. Li, C. C. Ko, G. P. Duan, N. Y. Zhu and V. W. W. Yam, *Organometallics*, 2007, **26**, 6091.
- C. D. McCaig, A. M. Rajnicek, B. Song and M. Zhao, *Physiol. Rev.*, 2005, **85**, 943.

- 5 N. B. Yang, A. L. George Jr. and R. Horn, *Neuron*, 1996, **16**, 113.
- 6 A. L. Hodgkin and A. F. Huxley, *J. Physiol.*, 1952, **117**, 500.
- 7 (a) A. Ojida, T. Sakamoto, M. A. Inoue, S. H. Fujishima, G. Lippens and I. Hamachi, *J. Am. Chem. Soc.*, 2009, **131**, 6543; (b) T. Y. Cheng, Y. F. Xu, S. Y. Zhang, W. P. Zhu, X. H. Qian and L. P. Duan, *J. Am. Chem. Soc.*, 2008, **130**, 16160; (c) L. J. Jiao, J. L. Li, S. Z. Zhang, C. Wei, E. H. Hao, M. Grac and H. Vicente, *New J. Chem.*, 2009, **33**, 1888.
- 8 (a) A. Nierth, A. Y. Kobitski, G. U. Nienhaus and A. Jäschke, *J. Am. Chem. Soc.*, 2010, **132**, 2646; (b) S. Atilgan, T. Ozdemir and E. U. Akkaya, *Org. Lett.*, 2008, **10**, 4065.
- 9 T. A. Golovkova, D. V. Kozlov and D. C. Neckers, *J. Org. Chem.*, 2005, **70**, 5545.
- 10 (a) A. Loudet and K. Burgess, *Chem. Rev.*, 2007, **107**, 4891; (b) T. J. Crevier, B. K. Bennett, J. D. Soper, J. A. Bowman, A. Dehestani, D. A. Hrovat, S. Lovell, W. Kaminsky and J. M. Mayer, *J. Am. Chem. Soc.*, 2001, **123**, 1059.
- 11 G. Ulrich, R. Ziessel and A. Harriman, *Angew. Chem., Int. Ed.*, 2008, **47**, 1184.
- 12 (a) L. Prodi, F. Bolletta, M. Montalti and N. Zaccheroni, *Coord. Chem. Rev.*, 2000, **205**, 59; (b) S. S. Sun and A. J. Lees, *Coord. Chem. Rev.*, 2002, **230**, 171; (c) R. M. Máñez and F. Sancenón, *Chem. Rev.*, 2003, **103**, 4419.
- 13 (a) T. Gunnlaugsson, T. C. Lee and R. Parkesh, *Org. Biomol. Chem.*, 2003, **1**, 3265; (b) X. F. Guo, X. H. Qian and L. H. Jia, *J. Am. Chem. Soc.*, 2004, **126**, 2272.
- 14 (a) M. M. C. Lo and G. C. Fu, *J. Am. Chem. Soc.*, 2002, **124**, 4572; (b) J. T. Hunt, T. Mitt, R. Borzilleri, J. G. Brown, J. Fagnoli, B. Fink, W. C. Han, S. Mortillo, G. Vite, B. Wautlet, T. Wong, C. Yu, X. P. Zheng and R. Bhide, *J. Med. Chem.*, 2004, **47**, 4054.
- 15 M. Baruah, W. W. Qin, N. Basarić, W. M. D. Borggraeve and N. Boens, *J. Org. Chem.*, 2005, **70**, 4152.
- 16 K. Rurack, M. Kollmannsberger and J. Daub, *Angew. Chem., Int. Ed.*, 2001, **40**, 385.
- 17 J. N. Demas and G. A. Crosby, *J. Phys. Chem.*, 1971, **75**, 991.
- 18 A. P. Silva, H. Q. N. Gunaratne and T. E. Rice, *Angew. Chem., Int. Ed. Engl.*, 1996, **35**, 2116.
- 19 J. Bourson, J. Pouget and B. Valeur, *J. Phys. Chem.*, 1993, **97**, 4552.
- 20 G. M. Sheldrick, *SHELXL97: SHELX97, Programs for Crystal Structure Analysis Release 97-2*, University of Goettingen, Germany, 1997.
- 21 (a) Z. Shen, H. Röhr, K. Rurack, H. Uno, M. Spieles, B. Schulz, G. Reck and N. Ono, *Chem.–Eur. J.*, 2004, **10**, 4853; (b) Y. H. Yu, A. B. Descalzo, Z. Shen, H. Röhr, Q. Liu, Y. W. Wang, M. Spieles, Y. Z. Li, K. Rurack and X. Z. You, *Chem.–Asian J.*, 2006, **1**, 176; (c) Q. D. Zheng, G. X. Xu and P. N. Prasad, *Chem.–Eur. J.*, 2008, **14**, 5812.
- 22 (a) M. Baruah, W. W. Qin, C. Flors, J. Hofkens, R. A. L. Vallée, D. Beljonne, M. V. D. Auweraer, W. M. D. Borggraeve and N. Boens, *J. Phys. Chem. A*, 2006, **110**, 5998; (b) W. W. Qin, M. Baruah, M. Sliwa, M. V. D. Auweraer, W. M. D. Borggraeve, D. Beljonne, B. V. Averbeke and N. Boens, *J. Phys. Chem. A*, 2008, **112**, 6104.
- 23 E. Lippert, *Z. Naturforsch., A: Phys. Sci.*, 1955, **10**, 541.
- 24 A. Coskun, E. Deniz and E. U. Akkaya, *Org. Lett.*, 2005, **7**, 5187.